ASME Journal of Applied Mechanics
Online journal at:
https://asmedigitalcollection.asme.org/appliedmechanics

An Electro-Chemo-Mechanical Theory With Flexoelectricity: Application to Ionic Conductivity of Soft Solid Electrolytes

Anand Mathew
Department of Mechanical Engineering,
University of Houston,
Houston, TX 77204
e-mail: amathe28@CougarNet.UH.EDU

Yashashree Kulkarni[1]
Department of Mechanical Engineering,
University of Houston,
Houston, TX 77204
e-mail: ykulkarni@uh.edu

Flexible batteries are gaining momentum in several fields, including wearable medical devices and biomedical sensors, flexible displays, and smartwatches. These energy storage devices are subjected to electro-chemo-mechanical effects. Here, we present a theoretical framework that couples diffusion and electromechanical theory with flexoelectricity. As an example, we investigate the effect of flexoelectricity on the ionic conductivity in soft materials. Our analytical results for a thin film made of a soft material reveal that the ionic conductivity is significantly higher at the nanoscale and decreases exponentially to approach the bulk value with increasing film thickness. Furthermore, we find that flexoelectricity reduces the ionic conductivity dramatically at film thickness smaller than the length scale associated with flexoelectricity. This behavior is attributed to the opposite directions of polarization induced by flexoelectricity and the flow of ions driven by the chemical potential. These findings shed light on the interplay between flexoelectricity and diffusion which would be paramount in designing miniaturized energy storage devices.
[DOI: 10.1115/1.4063897]

Keywords: constitutive modeling of materials, elasticity, mechanical properties of materials

1 Introduction

In the rapidly evolving world of technology, energy storage devices are playing an increasingly vital role [1,2]. This is due to the dramatic increase in demand for miniature self-powering devices, flexible dynamic displays, portable electronics, health care, and fitness-tracking devices, among others [3,4]. The key components of batteries that govern their efficiency as energy storage devices are the electrodes and the electrolyte. Naturally then, there has been tremendous activity in the areas of materials science and mechanics in understanding and improving the mechanical behavior of the electrodes [5–10] and electrolytes [11–14]. The electrolyte facilitates the flow of ions between the electrodes and enables the chemical reactions that generate electrical energy, making the battery functional. Ionic conductivity of electrolytes is an essential characteristic as it determines the efficiency and performance of a battery. Conventional Li-ion batteries work by ionic transport between two electrodes through a non-aqueous liquid electrolyte [15,16]. Although these energy storage devices have high ionic conductivity [17] which leads to rapid charge and discharge rates, they do not support large deformations which are imperative for designing stretchable and flexible batteries. This is where solid-state batteries show extraordinary promise which has led to a surge of interest in stretchable and flexible solid-state batteries with solid electrolytes [18–20].

Solid-state batteries with solid electrolytes offer significant advantages over traditional Li-ion batteries, despite their lower ionic conductivity. They not only have a higher energy density [21] but also exhibit superior thermal stability [22], making them an ideal choice for miniature wearable technologies. In addition, solid-state batteries are a safer alternative to Li-ion batteries, as they eliminate the risk of organic solvent leakage [23], which could be toxic. Solid electrolytes also inhibit the growth of lithium dendrites [24], enhancing their overall safety and performance. Particularly in the context of stretchable and flexible batteries, electrolytes that are solid-state as well as soft are ideal candidates. Interestingly, in soft solid electrolytes, the strain gradients resulting from bending and twisting induce a flexoelectric effect, which is further compounded by the presence of ionic diffusion. This interaction between strain gradients and ionic diffusion highlights the importance of studying the coupling of these two effects in soft or flexible solid-state batteries. We refer the reader to a perspective article by Ardebili on the mechanics issues in soft solid electrolytes [25].

Flexoelectricity is the phenomenon that arises due to the coupling between strain gradient and polarization. Unlike piezoelectricity which is another form of electromechanical coupling between uniform strain and polarization that only exists in

[1]Corresponding author.

Contributed by the Applied Mechanics Division of ASME for publication in the Journal of Applied Mechanics. Manuscript received October 7, 2023; final manuscript received October 23, 2023; published online November 16, 2023. Tech. Editor: Pradeep Sharma.

noncentrosymmetric crystals, flexoelectricity in principle exists in all dielectric/insulating materials [26]. The mathematical expression for polarization due to piezoelectricity and flexoelectricity is given by [27]

$$P_i = d_{ijk}\varepsilon_{jk} + f_{ijkl}\frac{\partial \varepsilon_{jk}}{\partial x_l} \tag{1}$$

Here, P_i is the component of the polarization vector, ε_{jk} is the component of strain, d_{ijk} and f_{ijkl} are the components of third-order piezoelectric tensor and fourth-order flexoelectric tensor, respectively. Flexoelectricity is predominant in soft materials [27–29], nanomaterials [26], and materials where traditional electromechanical couplings (e.g., piezoelectricity) are absent. Flexoelectricity has been widely studied in the biological context [27,30–35] and in liquid crystals [36,37]. With the advent of soft solid electrolytes for next-generation solid-state batteries, it is critical to understand the mechanics of soft materials subjected to mechanical, chemical, and electrical effects as well as their coupling. To this end, in this paper,

- We formulate a multi-physics theory incorporating diffusion and flexoelectricity for soft materials rooted in the principles of thermodynamics and continuum mechanics. The resulting governing equations enable an understanding of the coupling between the two phenomena.
- By solving a boundary value problem of a soft thin film, we investigate the variation of ionic conductivity as a function of film thickness and stain under the effect of flexoelectricity and diffusion of ions.
- We determine the effect on the overall polarization across the thin film due to the coupling of diffusion with flexoelectricity and provide insights into the interplay between the two effects on the ionic conductivity in the thin film.

The outline of the paper is as follows. In Sec. 2, we present a comprehensive continuum theory that couples the effect due to flexoelectricity and diffusion. We intend to derive the governing equations and the associated boundary conditions. In Sec. 3, the governing equations and boundary conditions for the thin film are derived, and the equations are solved numerically. In Sec. 4, we analyze and discuss the results to elucidate the significant effects of the coupling of flexoelectricity and diffusion on the behavior of the polymer thin film and its implications for ionic conductivity. In Sec. 5, we conclude by summarizing the key results of the paper and discussing avenues for future studies.

2 A Nonlinear Continuum Theory for Electromechanical Coupling and Diffusion

In this section, we develop a theoretical framework for electro-elastic-diffusive solids incorporating flexoelectricity. Specifically, we present a nonlinear continuum theory for flexoelectricity coupled with diffusion. A theoretical framework for modeling electro-elastic-diffusive systems without considering the effect of flexoelectricity was proposed by Mozaffari et al. [38]. A continuum theory of flexoelectricity was developed by Deng et al. [39]. We will closely follow these two works in formulating an integrated continuum theory for electromechanical coupling and diffusion in soft materials.

Notations: Uppercase and lowercase denote parameters in the reference and current configuration, respectively, unless specified otherwise. ∇_y, div, curl, and grad denote differential operators in the current configuration and ∇, Div, Curl, and Grad denote the differential operators in the reference configuration.

2.1 System Definition. As shown in Fig. 1, we consider a continuum body undergoing elastic deformation coupled with diffusion of ions in the presence of an electric field. The thermodynamic state of the system is then determined by the deformation $\mathbf{y}(.,\ t)\ :\ \Omega_R \to \Omega(t)$, ion volumetric concentration $c(.,\ t):\Omega_R \to \mathbb{R}$, and polarization $\mathbf{P}(.,\ t):\Omega_R \to \mathbb{R}^3$. Here, Ω_R denotes the reference configuration and $\Omega(t)$ denotes the current configuration.

The behavior of the continuum body is consistent with the laws of thermodynamics and Maxwell equations:

$$\nabla \times \mathbf{e} = 0 \quad \text{and} \quad \nabla \cdot \mathbf{d} = \rho_f^c \tag{2}$$

where ρ_f^c is the free charge density, $\mathbf{e}$ is the electric field, and $\mathbf{d}$ is the electric displacement in the current configuration. The polarization in the current configuration is given by

$$\mathbf{p} = \mathbf{d} - \varepsilon_0 \mathbf{e} \tag{3}$$

The continuum body interacts with the ambient system through a set of mechanical, chemical, and electrical boundary conditions. The mechanical boundary conditions are imposed on the subdivisions S_D and S_N of $\partial\Omega_R$ as follows:

$$\begin{cases} \mathbf{y}(\mathbf{x},\ t) = \mathbf{y}_b(\mathbf{x},\ t) & \text{on} \quad S_D \\ \text{applied external traction} = \mathbf{t}^e(\mathbf{x},\ t) & \text{on} \quad S_N \end{cases} \tag{4}$$

where $\mathbf{y}_b(.,\ t):S_D \to \mathbb{R}^3$ is the prescribed boundary position in the current configuration. The chemical boundary conditions are imposed on the subdivisions Υ_D and Υ_N of $\partial\Omega_R$ as follows:

$$\begin{cases} \mu = \mu^e(\mathbf{x},\ t) & \text{on} \quad \Upsilon_D \\ \mathbf{J}(\mathbf{x},\ t)\cdot\mathbf{n} = J^e & \text{on} \quad \Upsilon_N \end{cases} \tag{5}$$

where $\mu(.,\ t):\Upsilon_D \to \mathbb{R}$ is the chemical potential, and $\mu^e(.,\ t)$ is the prescribed chemical potential on Υ_D. $\mathbf{J}(.,\ t):\Omega_R \to \mathbb{R}^3$ is the ionic flux and J^e is the prescribed flux perpendicular to the boundary on Υ_N. As illustrated in Fig. 1, an electric field is applied by an external circuit. The electric field, denoted by ξ: $\Omega_R \to \mathbb{R}$, has an effect on the transport of ions in the electrolyte. Assuming the boundary potential applied by the external circuit to be ξ^e on Υ_D, we get the electrical boundary condition as follows:

$$\xi = \xi^e(\mathbf{x}) \quad \text{on} \quad \Upsilon_D \tag{6}$$

2.2 Balance Law for Species Diffusion. The derivation in this section is similar to Ref. [40]. Let $c(\mathbf{x},\ t)$ be the total number of moles of the diffusing species per unit volume in the reference configuration. The diffusing species can also be characterized by the species flux, $\mathbf{J}(\mathbf{x},\ t)$, through the reference outer boundary $\partial\Omega_R^+$. The number of moles of species per unit area per unit time is given by

$$\int_{\partial\Omega_R^+} J^e = -\int_{\partial\Omega_R^+} \mathbf{J}(\mathbf{x},\ t)\cdot\mathbf{n} \tag{7}$$

The rate of chemical species across the volume, Ω_R, is given by

$$\int_{\Omega_R} \dot{c} = -\int_{\partial\Omega_R^+} \mathbf{J}\cdot\mathbf{n} \tag{8}$$

Applying the divergence theorem, we get the equation for species mass balance:

$$\int_{\Omega_R} \dot{c} = -\int_{\Omega_R} \mathrm{Div}\mathbf{J} \tag{9}$$

Since Ω_R is arbitrary, the local form of species balance is given by

$$\dot{c} + \mathrm{Div}\mathbf{J} = 0 \quad \text{in} \quad \Omega_R \tag{10}$$

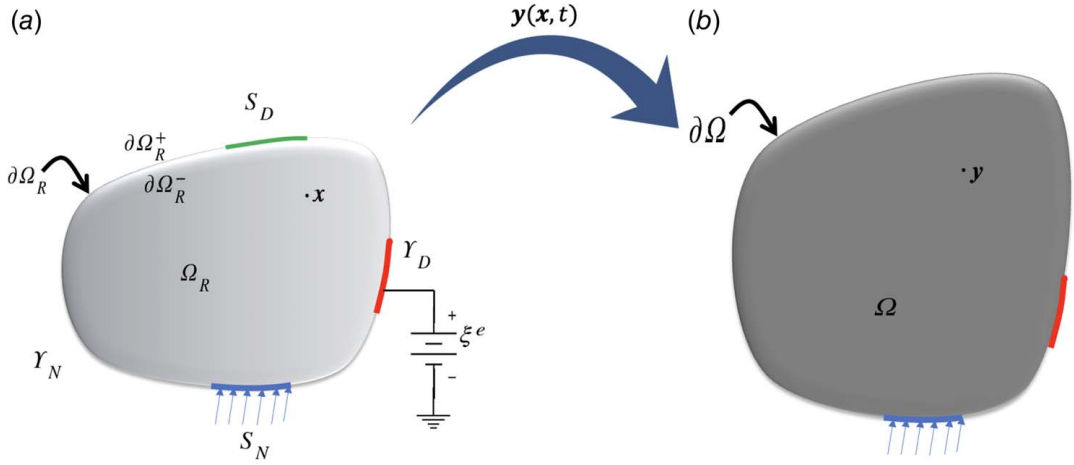

Fig. 1 An electro-elastic-diffusive continuum body in (*a*) reference and (*b*) current configuration. It is subjected to prescribed displacement on S_D and traction on S_N where $S_N \cup S_D = \partial\Omega_R$ and $S_N \cap S_D = \varnothing$. Υ_D is connected to a solution of ions whereas a flux is applied perpendicular to Υ_N where $\Upsilon_N \cup \Upsilon_D = \partial\Omega$ and $\Upsilon_N \cap \Upsilon_D = \varnothing$.

2.3 Rate of External Work. The rate of work done on the body has a contribution from mechanical, electrical, and chemical work. This can be expressed as

$$\dot{W} = \dot{W}_{\text{mech}} + \dot{W}_{\text{chem}} + \dot{W}_{\text{elec}} \tag{11}$$

where the individual terms are given as

$$\dot{W}_{\text{mech}} = \int_{\partial\Omega_R^+} \dot{\mathbf{y}} \cdot \mathbf{t}^e \tag{12}$$

$$\dot{W}_{\text{chem}} = -\int_{\partial\Omega_R^+} \mu^e (\mathbf{J} \cdot \mathbf{n}) \tag{13}$$

$$\dot{W}_{\text{elec}} = -\int_{\partial\Omega_R^+} q\xi^e (\mathbf{J} \cdot \mathbf{n}) - \int_{\partial\Omega_R^-} \xi(\dot{\mathbf{D}} \cdot \mathbf{n}) \tag{14}$$

Here, $\mathbf{D}$ is the nominal electric displacement which is given by

$$\mathbf{D} = -\varepsilon_0 \mathbf{J}\mathbf{C}^{-1}\nabla\xi + \mathbf{F}^{-1}\mathbf{P} \tag{15}$$

where $\mathbf{F} \equiv \nabla\mathbf{y}$ is the deformation gradient and $\mathbf{C}$ is the right Cauchy–Green deformation tensor. $\partial\Omega_R^+$ is the exterior boundary of $\partial\Omega_R$ and $\partial\Omega_R^-$ is the interior boundary of $\partial\Omega_R$. Thus, Eq. (12) is the rate of work done by the applied traction on the external surface of the continuum body in the reference configuration. The first term in Eqs. (13) and (14) is associated with the chemical flux and electrical flux, respectively, due to the flow of ions into the continuum body. These terms have a negative sign because the direction of flux and normal are opposite to each other. We note that the electric potential, ξ, may be discontinuous because of the presence of chemical potential. The second term in Eq. (14) can be interpreted considering the body as a capacitor. Thus, consistent with Ref. [38], the total rate of work done on the body is

$$\dot{W} = \int_{\partial\Omega_R^+} \dot{\mathbf{y}} \cdot \mathbf{t}^e - \int_{\partial\Omega_R^+} \left(\mu^e + q\xi^e\right)(\mathbf{J} \cdot \mathbf{n}) - \int_{\partial\Omega_R^-} \xi(\dot{\mathbf{D}} \cdot \mathbf{n}) \tag{16}$$

2.4 Rate of Change of Free Energy. We postulate that the free energy of the body is given by

$$U[\mathbf{y}, c] = U_b[\mathbf{y}, c] + U_{\text{elect}}[\mathbf{y}, c] \tag{17}$$

where U_{elect} is the energy associated with the charges whereas U_b includes a contribution to the free energy from deformation, diffusion, and electromechanical coupling. Below, we derive expressions for the rate of change of U_b and U_{elect}.

2.4.1 Rate of Change of U_b. We postulate that the Helmholtz free energy density, Ψ, defines the constitutive behavior of the body undergoing a quasi-static isothermal process and has the form

$$U_b[\mathbf{y}, c] = \int_{\Omega_R} \Psi(\mathbf{F}, \mathbf{G}, \mathbf{P}, \mathbf{\Pi}, c, \boldsymbol{\kappa}) \tag{18}$$

where $\mathbf{G}$ is the gradient of $\mathbf{F}$, $\mathbf{\Pi}$ is the gradient of polarization, and $\boldsymbol{\kappa}$ is the gradient of concentration. The free energy combines the energy postulated by Deng et al. [39] for flexoelectricity and by Mozaffari et al. [38] for an electro-elastic-diffusive system without flexoelectricity.

From the principle of material frame indifference and from material symmetries, we have

$$\begin{cases} \Psi(\mathbf{RF}, \mathbf{RG}, \mathbf{RP}, \mathbf{R\Pi}, c, \mathbf{R}\boldsymbol{\kappa}) = \Psi(\mathbf{F}, \mathbf{G}, \mathbf{P}, \mathbf{\Pi}, c, \boldsymbol{\kappa}) & \forall\, \mathbf{R} \in SO(3) \\ \Psi(\mathbf{FQ}, \mathbf{GQ}, \mathbf{PQ}, \mathbf{\Pi Q}, c, \boldsymbol{\kappa}\mathbf{Q}) = \Psi(\mathbf{F}, \mathbf{G}, \mathbf{P}, \mathbf{\Pi}, c, \boldsymbol{\kappa}) & \forall\, \mathbf{Q} \in \mathcal{G} \end{cases} \tag{19}$$

Here, $SO(3)$ is the set of all rigid rotations and $\mathcal{G} \subset SO(3)$ is the group associated with material symmetries. If a material is isotropic, $\mathcal{G} = SO(3)$. Since c is a scalar and $\mathbf{J}$ is a referential vector field, they are both material frame indifferent.

Then, the time derivative of Eq. (18) yields

$$\dot{U}_b = \int_{\Omega_R} \frac{\mathrm{d}}{\mathrm{d}t} \Psi(\mathbf{F}, \mathbf{G}, \mathbf{P}, \mathbf{\Pi}, c, \boldsymbol{\kappa}) \tag{20}$$

$$= \int_{\Omega_R} \frac{\partial\Psi}{\partial\mathbf{F}} \cdot \nabla\dot{\mathbf{y}} + \frac{\partial\Psi}{\partial\mathbf{G}} \cdot \nabla\nabla\dot{\mathbf{y}} + \frac{\partial\Psi}{\partial\mathbf{P}} \cdot \dot{\mathbf{P}} + \frac{\partial\Psi}{\partial\mathbf{\Pi}} \cdot \dot{\mathbf{\Pi}} + \frac{\partial\Psi}{\partial c} \cdot \dot{c} + \frac{\partial\Psi}{\partial\boldsymbol{\kappa}} \cdot \dot{\boldsymbol{\kappa}} \tag{21}$$

We note that

$$\boldsymbol{\sigma} \equiv \frac{\partial\Psi}{\partial\mathbf{F}} \quad \text{and} \quad \mu \equiv \frac{\partial\Psi}{\partial c} \tag{22}$$

where $\boldsymbol{\sigma}$ is the local internal Piola–Kirchhoff stress and μ is the chemical potential. We use the balance law for species diffusion to manipulate the last two terms in Eq. (21) and use the divergence theorem to simplify the remaining terms as follows:

$$\int_{\Omega_R}\frac{\partial\Psi}{\partial\mathbf{F}}\cdot\nabla\dot{\mathbf{y}}=\int_{\partial\Omega_R^-}(\boldsymbol{\sigma}\cdot\mathbf{n})\dot{\mathbf{y}}-\int_{\Omega_R}\mathrm{Div}(\boldsymbol{\sigma})\cdot\dot{\mathbf{y}}$$
$$\int_{\Omega_R}\frac{\partial\Psi}{\partial\mathbf{G}}\cdot\nabla\nabla\dot{\mathbf{y}}=\int_{\partial\Omega_R^-}\left(\left(\frac{\partial\Psi}{\partial\mathbf{G}}\right)\cdot\mathbf{n}\right)\nabla\dot{\mathbf{y}}-\int_{\partial\Omega_R^-}\left(\mathrm{Div}\left(\frac{\partial\Psi}{\partial\mathbf{G}}\right)\cdot\mathbf{n}\right)\dot{\mathbf{y}}\int_{\Omega_R}\mathrm{Div}\left(\mathrm{Div}\left(\frac{\partial\Psi}{\partial\mathbf{G}}\right)\right)\cdot\dot{\mathbf{y}}$$
$$\int_{\Omega_R}\frac{\partial\Psi}{\partial\boldsymbol{\Pi}}\cdot\dot{\boldsymbol{\Pi}}=\int_{\partial\Omega_R^-}\left(\frac{\partial\Psi}{\partial\boldsymbol{\Pi}}\cdot\mathbf{n}\right)\dot{\mathbf{P}}-\int_{\Omega_R}\mathrm{Div}\left(\frac{\partial\Psi}{\partial\boldsymbol{\Pi}}\right)\cdot\dot{\mathbf{P}}$$
$$\int_{\Omega_R}\frac{\partial\Psi}{\partial c}\cdot\dot{c}=-\int_{\Omega_R}\mu(\mathrm{Div}\mathbf{J})=\int_{\Omega_R}\mathbf{J}\cdot\nabla\mu-\int_{\partial\Omega_R^-}(\mathbf{J}\cdot\mathbf{n})\mu$$
$$\int_{\Omega_R}\frac{\partial\Psi}{\partial\boldsymbol{\kappa}}\cdot\dot{\boldsymbol{\kappa}}=-\int_{\partial\Omega_R^-}\mathrm{Div}\left(\frac{\partial\Psi}{\partial\boldsymbol{\kappa}}\right)(\mathbf{J}\cdot\mathbf{n})+\int_{\Omega_R}\mathbf{J}\cdot\mathrm{Grad}\left(\mathrm{Div}\left(\frac{\partial\Psi}{\partial\boldsymbol{\kappa}}\right)\right)+\int_{\partial\Omega_R^-}\left(\frac{\partial\Psi}{\partial\boldsymbol{\kappa}}\cdot\mathbf{n}\right)\mathrm{Div}\mathbf{J}\tag{23}$$

The first term of Eq. $(23)_2$ can be further reduced to

$$\begin{aligned}\int_{\partial\Omega_R^-}\left(\left(\frac{\partial\Psi}{\partial\mathbf{G}}\right)\cdot\mathbf{n}\right)\nabla\dot{\mathbf{y}}&=\int_{\partial\Omega_R^-}\left[\left(\frac{\partial\Psi}{\partial\mathbf{G}}\right)\mathbf{n}\otimes(\mathbf{I}-\mathbf{n}\otimes\mathbf{n})+\frac{\partial\Psi}{\partial\mathbf{G}}\mathbf{n}\otimes\mathbf{n}\otimes\mathbf{n}\right]\nabla\dot{\mathbf{y}}\,\mathrm{d}A\\&=\int_{\partial\Omega_R^-}\mathrm{Div}\left(\left(\frac{\partial\Psi}{\partial\mathbf{G}}\right)(\mathbf{n}\otimes(\mathbf{I}-\mathbf{n}\otimes\mathbf{n}))\dot{\mathbf{y}}\right)-\int_{\partial\Omega_R^-}\mathrm{Div}\left(\left(\frac{\partial\Psi}{\partial\mathbf{G}}\right)\mathbf{n}\otimes(\mathbf{I}-\mathbf{n}\otimes\mathbf{n})\right)\dot{\mathbf{y}}+\int_{\partial\Omega_R^-}\mathrm{Div}\left(\frac{\partial\Psi}{\partial\mathbf{G}}\right)(\mathbf{n}\otimes\mathbf{n})(\dot{\mathbf{y}}\cdot\mathbf{n})\end{aligned}\tag{24}$$

For any vector $\mathbf{V}$ on a closed boundary $\partial\Omega_R^-$, the tangential component of $\nabla\dot{\mathbf{y}}$ is independent of $\dot{\mathbf{y}}$ since [38]

$$\int_{\partial\Omega_R^-}(\mathrm{Div}\mathbf{V}):(\mathbf{I}-\mathbf{n}\otimes\mathbf{n})=0\tag{25}$$

Then, the first term of Eq. (24) becomes zero. Denoting $(\partial\Psi/\partial\mathbf{G})\mathbf{n}\otimes(\mathbf{I}-\mathbf{n}\otimes\mathbf{n})$ by a tensor $\boldsymbol{\beta}$, we get the rate of change of free energy of the body by substituting Eqs. (23) and (24) in Eq. (20) as follows:

$$\begin{aligned}\dot{U}_b=&\int_{\partial\Omega_R^-}\mathrm{Div}\left(\frac{\partial\Psi}{\partial\mathbf{G}}\right)(\mathbf{n}\otimes\mathbf{n})(\dot{\mathbf{y}}\cdot\mathbf{n})+\int_{\partial\Omega_R^-}\left[\left[\boldsymbol{\sigma}-\mathrm{Div}\left(\frac{\partial\Psi}{\partial\mathbf{G}}\right)\right]\cdot\mathbf{n}-\mathrm{Div}\boldsymbol{\beta}\right]\dot{\mathbf{y}}+\int_{\partial\Omega_R^-}\left(\frac{\partial\Psi}{\partial\boldsymbol{\Pi}}\cdot\mathbf{n}\right)\dot{\mathbf{P}}\\&+\int_{\Omega_R}\mathrm{Div}\left[\boldsymbol{\sigma}-\mathrm{Div}\left(\frac{\partial\Psi}{\partial\mathbf{G}}\right)\right]\cdot\dot{\mathbf{y}}+\int_{\Omega_R}\left[\frac{\partial\Psi}{\partial\mathbf{P}}-\mathrm{Div}\left(\frac{\partial\Psi}{\partial\boldsymbol{\Pi}}\right)\right]\cdot\dot{\mathbf{P}}+\int_{\Omega_R}\mathbf{J}\cdot\nabla\mu-\int_{\partial\Omega_R^-}(\mathbf{J}\cdot\mathbf{n})\mu\\&-\int_{\partial\Omega_R^-}\mathrm{Div}\left(\frac{\partial\Psi}{\partial\boldsymbol{\kappa}}\right)(\mathbf{J}\cdot\mathbf{n})+\int_{\Omega_R}\mathbf{J}\cdot\mathrm{Grad}\left(\mathrm{Div}\left(\frac{\partial\Psi}{\partial\boldsymbol{\kappa}}\right)\right)+\int_{\partial\Omega_R^-}\left(\frac{\partial\Psi}{\partial\boldsymbol{\kappa}}\cdot\mathbf{n}\right)\mathrm{Div}\mathbf{J}\end{aligned}\tag{26}$$

2.4.2 Rate of Change of U_{elect}. The calculations presented here follow the work of Darbaniyan et al. [41]. The electric energy in the current configuration is given by

$$U_{\text{elect}}=\int_{\Omega}\frac{\varepsilon_0}{2}|\nabla_y\xi|^2\,\mathrm{d}v\tag{27}$$

where ε_0 is the permittivity of free space. Converting Eq. (27) to the reference configuration, we get

$$U_{\text{elect}}=\int_{\Omega_R}\frac{\varepsilon_0}{2}J|\mathbf{F}^{-T}\nabla\xi|^2\,\mathrm{d}V\tag{28}$$

where we recall that $\nabla_y\xi=\mathbf{F}^{-T}\nabla\xi$ and $\mathrm{d}v=J\,\mathrm{d}V$, J is the Jacobian. Using standard results from continuum mechanics [41]

$$\dot{\mathbf{F}}^{-1}=-\mathbf{F}^{-1}\dot{\mathbf{F}}\mathbf{F}^{-1}\tag{29}$$

$$\dot{J}=J\mathbf{F}^{-T}\cdot\dot{\mathbf{F}}\tag{30}$$

$$\dot{\overline{J\mathbf{C}^{-1}}}=-J\mathbf{F}^{-1}\dot{\mathbf{F}}\mathbf{F}^{-T}-J\mathbf{C}^{-1}\dot{\mathbf{F}}^T\mathbf{F}^{-T}+J(\mathbf{F}^{-T}\cdot\dot{\mathbf{F}})\mathbf{C}^{-1}\tag{31}$$

we get

$$\frac{\varepsilon_0}{2}\nabla\xi\cdot\dot{\overline{J\mathbf{C}^{-1}}}\nabla\xi=-\varepsilon_0J\dot{\mathbf{F}}\cdot\left[(\mathbf{F}^{-T}\nabla\xi)\otimes(\mathbf{C}^{-1}\nabla\xi)-\frac{1}{2}|\mathbf{F}^{-T}\nabla\xi|\mathbf{F}^{-T}\right]\tag{32}$$

Taking the time derivative of Eq. (28) and using the divergence theorem, we get

$$\dot{U}_{\text{elect}}=\int_{\Omega_R}\left[\nabla\dot{\mathbf{y}}\cdot\boldsymbol{\Sigma}_{MW}+\nabla\xi\cdot\mathbf{F}^{-1}\dot{\mathbf{P}}+\xi(\nabla\cdot\dot{\mathbf{D}})\right]-\int_{\partial\Omega_R^-}\xi(\dot{\mathbf{D}}\cdot\mathbf{n})\tag{33}$$

where $\boldsymbol{\Sigma}_{MW}$ is the Maxwell stress expressed as

$$\boldsymbol{\Sigma}_{MW}[\mathbf{F},\mathbf{P}]=(\mathbf{F}^{-T}\nabla\xi)\otimes(\varepsilon_0J\mathbf{C}^{-1}\nabla\xi-\mathbf{F}^{-1}\mathbf{P})-\frac{\varepsilon_0}{2}|\mathbf{F}^{-T}\nabla\xi|\mathbf{F}^{-T}\tag{34}$$

Using Eq. (15) and the Maxwell equation, $\mathrm{Div}\mathbf{D}=\rho_f$, where ρ_f is the free charge density in the reference configuration, we get

$$\mathrm{Div}\mathbf{D}=q(c-c_0(\mathbf{x}))\tag{35}$$

where c_0 is the concentration of immobile ions. Taking the time

derivative, we get

$$\nabla \cdot \dot{\mathbf{D}} = q\dot{c} \tag{36}$$

Using the Maxwell equation, $\mathbf{J}_e + \dot{\mathbf{D}} = 0$, ignoring magnetic effects, we get

$$\dot{\mathbf{D}} = -\mathbf{J}_e = -q\mathbf{J} \tag{37}$$

where $\mathbf{J}_e$ is the electric current density in the reference configuration. Using Eqs. (36) and (37) in Eq. (33) yields

$$\dot{U}_{\text{elect}} = \int_{\Omega_R} \left[\nabla\dot{\mathbf{y}} \cdot \boldsymbol{\sigma}_{MW} + \nabla\xi \cdot \mathbf{F}^{-1}\dot{\mathbf{P}} + q\dot{c}\xi\right] + \int_{\partial\Omega_R^-} q\xi(\mathbf{J}\cdot\mathbf{n}) \tag{38}$$

Applying the divergence theorem to the first and last terms, we get

$$\dot{U}_{\text{elect}} = \int_{\Omega_R} \left[-\dot{\mathbf{y}} \cdot \text{Div}(\boldsymbol{\sigma}_{MW}) + (\mathbf{F}^{-T} \cdot \nabla\xi)\dot{\mathbf{P}} + \mathbf{J} \cdot \nabla(q\xi)\right] + \int_{\partial\Omega_R^-} \dot{\mathbf{y}}(\boldsymbol{\sigma}_{MW} \cdot \mathbf{n}) \tag{39}$$

2.5 Rate of Energy Dissipation. The rate of energy dissipation is given by

$$\dot{D} = \dot{W} - \dot{U}_b - \dot{U}_{\text{elect}} \tag{40}$$

Substituting Eqs. (16), (26), and (39) in Eq. (40), we get the expression for the rate of energy dissipation as

$$\begin{aligned}\dot{D} = &\int_{\Omega_R} \text{Div}\left[\boldsymbol{\sigma} - \text{Div}\left(\frac{\partial\Psi}{\partial\mathbf{G}}\right) + \boldsymbol{\sigma}_{MW}\right] \cdot \dot{\mathbf{y}} - \int_{\Omega_R} \mathbf{J} \cdot \nabla(q\xi + \mu) - \int_{\Omega_R} \left[\frac{\partial\Psi}{\partial\mathbf{P}} - \text{Div}\left(\frac{\partial\Psi}{\partial\boldsymbol{\Pi}}\right) + \mathbf{F}^{-T} \cdot \nabla\xi\right] \cdot \dot{\mathbf{P}} - \int_{\partial\Omega_R^+} (\mu^e + q\xi^e)(\mathbf{J}\cdot\mathbf{n}) \\ &+ \int_{\partial\Omega_R^-} (\mu + q\xi)(\mathbf{J}\cdot\mathbf{n}) + \int_{\partial\Omega_R^+} \dot{\mathbf{y}} \cdot \mathbf{t}^e - \int_{\partial\Omega_R^-} \left(\frac{\partial\Psi}{\partial\boldsymbol{\Pi}} \cdot \mathbf{n}\right)\dot{\mathbf{P}} + \int_{\partial\Omega_R^-} \text{Div}\left(\frac{\partial\Psi}{\partial\boldsymbol{\kappa}}\right)(\mathbf{J}\cdot\mathbf{n}) - \int_{\Omega_R} \mathbf{J} \cdot \text{Grad}\left(\text{Div}\left(\frac{\partial\Psi}{\partial\boldsymbol{\kappa}}\right)\right) - \int_{\partial\Omega_R^-} \left(\frac{\partial\Psi}{\partial\boldsymbol{\kappa}} \cdot \mathbf{n}\right)\text{Div}\mathbf{J} \\ &- \int_{\partial\Omega_R^-} \left[\left(\boldsymbol{\sigma} - \text{Div}\left(\frac{\partial\Psi}{\partial\mathbf{G}}\right) + \boldsymbol{\sigma}_{MW}\right) \cdot \mathbf{n} - \text{Div}\boldsymbol{\beta}\right] \cdot \dot{\mathbf{y}} - \int_{\partial\Omega_R^-} \left(\frac{\partial\Psi}{\partial\mathbf{G}}\right)(\mathbf{n}\otimes\mathbf{n})(\dot{\mathbf{y}}\cdot\mathbf{n})\end{aligned} \tag{41}$$

2.6 Governing Equations and Boundary Conditions. According to the second law of thermodynamics, $\dot{\mathbf{D}} \geq 0$ for all isothermal processes. We follow the Coleman–Noll procedure to ensure that the laws of thermodynamics are satisfied and obtain the following:

$$\begin{cases} -\mathbf{J} \cdot \nabla\left(q\xi + \mu + \text{Div}\left(\dfrac{\partial\Psi}{\partial\boldsymbol{\kappa}}\right)\right) \geq 0 & \text{in} \quad \Omega_R \\ \text{Div}\left[\boldsymbol{\sigma} - \text{Div}\left(\dfrac{\partial\Psi}{\partial\mathbf{G}}\right) + \boldsymbol{\sigma}_{MW}\right] = 0 & \text{in} \quad \Omega_R \\ \left[\dfrac{\partial\Psi}{\partial\mathbf{P}} - \text{Div}\left(\dfrac{\partial\Psi}{\partial\boldsymbol{\Pi}}\right) + \mathbf{F}^{-T} \cdot \nabla\xi\right] = 0 & \text{in} \quad \Omega_R \\ \text{Div}\mathbf{D} = \rho_f & \text{in} \quad \Omega_R \end{cases} \tag{42}$$

We note that Eq. $(42)_2$ is the mechanical equilibrium equation accounting for electromechanical coupling. Equation $(42)_3$ yields an additional equation required to solve for polarization. Equation $(42)_4$ is the Maxwell equation. The inequality in Eq. $(42)_1$ can be satisfied by assuming the constitutive relation for diffusion to be of the form

$$\mathbf{J} = c\mathbf{v}, \quad \mathbf{v} = -\gamma(\mathbf{x})\nabla\left(q\xi + \mu + \text{Div}\left(\frac{\partial\Psi}{\partial\boldsymbol{\kappa}}\right)\right) \tag{43}$$

where $\mathbf{v}$ is the linear mobility. Thus, Eq. $(42)_1$ recovers the diffusion equation for ion concentration, c. To summarize, the electromechanical-diffusive system should satisfy the following governing equations:

$$\begin{cases} \dot{c} + \text{Div}\mathbf{J} = 0, \quad \mathbf{J} = -c\gamma(\mathbf{x})\nabla\left(q\xi + \mu + \text{Div}\left(\dfrac{\partial\Psi}{\partial\boldsymbol{\kappa}}\right)\right) & \text{in } \Omega_R \\ \text{Div}\left[\boldsymbol{\sigma} - \text{Div}\left(\dfrac{\partial\Psi}{\partial\mathbf{G}}\right) + \boldsymbol{\sigma}_{MW}\right] = 0 & \text{in } \Omega_R \\ \left[\dfrac{\partial\Psi}{\partial\mathbf{P}} - \text{Div}\left(\dfrac{\partial\Psi}{\partial\boldsymbol{\Pi}}\right) + \mathbf{F}^{-T} \cdot \nabla\xi\right] = 0 & \text{in } \Omega_R \\ \text{Div}\mathbf{D} = \rho_f & \text{in } \Omega_R \end{cases} \tag{44}$$

and boundary conditions:

$$\begin{cases} \left(\boldsymbol{\sigma} - \text{Div}\left(\dfrac{\partial\Psi}{\partial\mathbf{G}}\right) + \boldsymbol{\sigma}_{MW}\right) \cdot \mathbf{n} - \mathbf{t}^e - \text{Div}\boldsymbol{\beta} = 0 & \text{on} \quad S_N \\ \dfrac{\partial\Psi}{\partial\boldsymbol{\Pi}} \cdot \mathbf{n} = 0 & \text{on} \quad \partial\Omega_R \\ \mu^e + q\xi^e = \mu + q\xi + \text{Div}\left(\dfrac{\partial\Psi}{\partial\boldsymbol{\kappa}}\right) & \text{on} \quad \Upsilon_D \\ \mathbf{J} \cdot \mathbf{n} = 0 & \text{on} \quad \partial\Omega_R \backslash \Upsilon_D \\ \dfrac{\partial\Psi}{\partial\boldsymbol{\kappa}} \cdot \mathbf{n} = 0 & \text{on} \quad \partial\Omega_R \\ \dfrac{\partial\Psi}{\partial\mathbf{G}}\mathbf{n}\otimes\mathbf{n} = 0 & \text{on} \quad \partial\Omega_R \end{cases} \tag{45}$$

3 Example of an Electro-elastic-diffusive System—A Soft Solid Electrolyte

The boundary value problem derived in Eqs. (44) and (45) represents a general three-dimensional nonlinear continuum theory incorporating diffusion and electromechanical coupling with

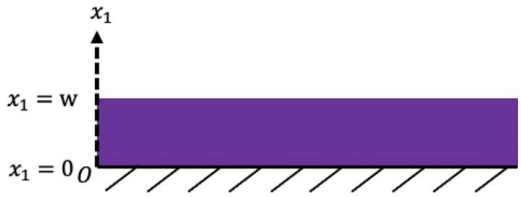

Fig. 2 Schematic of a polymer thin film of thickness w in the x_1 direction. The film is held fixed at $x_1 = 0$. This simplifies the boundary value problem to a 1D problem.

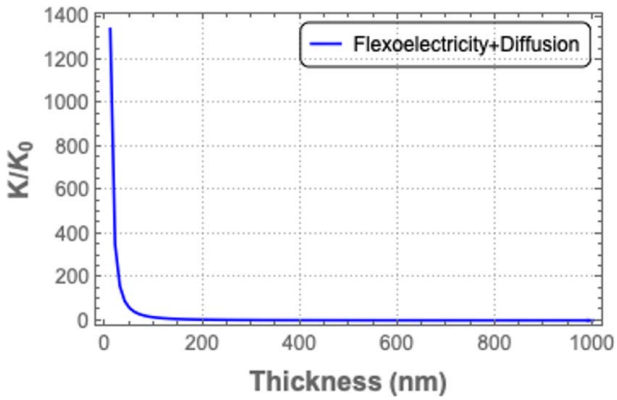

Fig. 3 Normalized ionic conductivity for varying thickness for a thin film subjected to 5% strain in an electro-elastic-diffusive system with flexoelectricity. The ionic conductivity is normalized by the conductivity at the initial concentration.

flexoelectricity. To demonstrate the coupled behavior of an electro-elastic-diffusive system, we consider a simple one-dimensional soft solid electrolyte as shown in Fig. 2. Our aim is to gain insights into the coupling between diffusion and electromechanical coupling. Specifically, we wish to elucidate the effect of flexoelectricity and the diffusion of ions on polarization and study their interplay in determining the ionic conductivity of electrolytes. Since electrostatics and flexoelectricity induce characteristic length scales into the problem, we will also investigate how ionic conductivity varies as a function of the film thickness.

3.1 Governing Equations. To this end, consider a thin film made of polyvinylidene fluoride (PVDF) with film thickness, w. For a linearized theory, we expand the Helmholtz free energy density Ψ up to quadratic terms to obtain

$$\begin{aligned}\Psi(\mathbf{F},\mathbf{G},\mathbf{P},\mathbf{\Pi},c;\mathbf{x}) = {}& \alpha_{el}(\mathbf{x})\mathrm{Tr}(\mathbf{F}-\mathbf{I}) + \frac{\beta(\mathbf{x})}{2}(c-c_0(\mathbf{x}))^2 \\ & + \hat{\mu}(\mathbf{x})(c-c_0(\mathbf{x})) + \frac{1}{2}\mathbf{P}\cdot\mathbf{a}(\mathbf{x})\mathbf{P} \\ & + \frac{1}{2}(\mathbf{F}-\mathbf{I}):\mathbb{C}(\mathbf{x})(\mathbf{F}-\mathbf{I}) + \mathbf{P}\cdot\mathbf{f}(\mathbf{x})\mathbf{G} \\ & + \frac{1}{2}\mathbf{\Pi}:\mathbf{b}(\mathbf{x})\mathbf{\Pi} + \mathbf{\Pi}:\mathbf{e}(\mathbf{x})(\mathbf{F}-\mathbf{I}) \end{aligned} \tag{46}$$

Here, $\mathbf{I}$ is the identity matrix, $\hat{\mu}(\mathbf{x})$ is the standard chemical potential or the chemical potential of the pure ion, $\alpha_{el}(\mathbf{x})$ is the coupling coefficient for elasto-diffusion, $\beta(\mathbf{x})$ is the chemistry modulus, $\mathbf{a}(\mathbf{x})$ is the reciprocal dielectric susceptibility, $\mathbb{C}(\mathbf{x})$ is the fourth-order elasticity tensor satisfying major and minor symmetries ($\mathbb{C}_{ijkl} = \mathbb{C}_{klij} = \mathbb{C}_{ijlk}$), $\mathbf{f}(\mathbf{x})$ is the fourth-order flexoelectric tensor, $\mathbf{b}(\mathbf{x})$ is the polarization gradient-polarization gradient coupling tensor, and $\mathbf{e}(\mathbf{x})$ is the coupling tensor corresponding to polarization gradient and strain proposed by Mindlin [42]. For the sake of simplicity, we have ignored the contribution from the concentration gradient, $\boldsymbol{\kappa}$, to the free energy. Finally, we note that the material properties are explicitly specified to be functions of $\mathbf{x}$. For brevity, in the subsequent calculations, this dependence on $\mathbf{x}$ will be tacitly assumed.

In our boundary value problem, we consider a classical electro-diffusion model known as the Poisson–Boltzmann–Nernst–Planck model [38,43]. Consistent with this model, we introduce the electrochemical potential and the Deybe length defined, respectively, as

$$\phi = \mu + q\xi \quad \text{and} \quad \lambda = \sqrt{\frac{\varepsilon_0\beta}{q^2}} \tag{47}$$

where q is the charge of the diffusing particle. From Eq. $(22)_2$, we get the relation

$$\mu = \alpha_{el}\nabla\cdot\mathbf{u} + \beta(c-c_0) + \hat{\mu} \tag{48}$$

which yields

$$c - c_0 = \frac{1}{\beta}\left(\mu - \hat{\mu} - \alpha_{el}\nabla\cdot\mathbf{u}\right) \tag{49}$$

Using Eqs. (47) and (49), the governing equations now take the form

$$\begin{cases} \dot{c} + \mathrm{Div}(-c\gamma\nabla\phi) = 0 & \text{in } \Omega_R \\ \mathrm{Div}\left[\dfrac{\partial\Psi}{\partial\mathbf{F}} - \mathrm{Div}\left(\dfrac{\partial\Psi}{\partial\mathbf{G}}\right) + \boldsymbol{\sigma}_{MW}\right] = 0 & \text{in } \Omega_R \\ \left[\dfrac{\partial\Psi}{\partial\mathbf{P}} - \mathrm{Div}\left(\dfrac{\partial\Psi}{\partial\mathbf{\Pi}}\right) + \mathbf{F}^{-T}\cdot\nabla\xi\right] = 0 & \text{in } \Omega_R \\ \mathrm{Div}\left(-J\mathbf{C}^{-1}\nabla\xi + \dfrac{1}{\varepsilon_0}\mathbf{F}^{-1}\mathbf{P}\right) + \dfrac{\xi}{\lambda^2} = \dfrac{q}{\varepsilon_0\beta}\left(\phi - \hat{\mu} - \alpha_{el}\nabla\cdot\mathbf{u}\right) & \text{in } \Omega_R \end{cases} \tag{50}$$

Assuming small strain with $|\nabla\mathbf{u}| \ll 1$, Eq. (50) can be further simplified. The Maxwell stress also vanishes under small deformation assumption [38,39]. This yields

$$\begin{cases} \dot{c} + \mathrm{Div}(-c\gamma\nabla\phi) = 0 & \text{in } \Omega_R \\ \mathrm{Div}\left[\dfrac{\partial\Psi}{\partial\mathbf{F}} - \mathrm{Div}\left(\dfrac{\partial\Psi}{\partial\mathbf{G}}\right)\right] = 0 & \text{in } \Omega_R \\ \left[\dfrac{\partial\Psi}{\partial\mathbf{P}} - \mathrm{Div}\left(\dfrac{\partial\Psi}{\partial\mathbf{\Pi}}\right) + \nabla\xi\right] = 0 & \text{in } \Omega_R \\ \mathrm{Div}\left(-\nabla\xi + \dfrac{1}{\varepsilon_0}\mathbf{P}\right) + \dfrac{\xi}{\lambda^2} = \dfrac{q}{\varepsilon_0\beta}\left(\phi - \hat{\mu} - \alpha_{el}\nabla\cdot\mathbf{u}\right) & \text{in } \Omega_R \end{cases} \tag{51}$$

For a thin film, we assume that the fields only vary in the thickness direction. Let the direction perpendicular to the film be x_1 as shown in Fig. 2. Substituting the one-dimensional Helmholtz free energy density (Eq. (46)) in Eq. (51), we arrive at the following simplified governing equations:

$$\begin{cases} \dot{c} + \dfrac{\mathrm{d}}{\mathrm{d}x_1}(-c\gamma\nabla\phi) = 0 & \text{in } \Omega_R \\ \left(\mathbb{C} - \dfrac{\alpha_{el}^2}{\beta}\right)\dfrac{\mathrm{d}^2u}{\mathrm{d}x_1^2} + h\dfrac{\mathrm{d}^2P}{\mathrm{d}x_1^2} + \dfrac{\alpha_{el}}{\beta}\dfrac{\mathrm{d}\mu}{\mathrm{d}x_1} = 0 & \text{in } \Omega_R \\ h\dfrac{\mathrm{d}^2u}{\mathrm{d}x_1^2} + b\dfrac{\mathrm{d}^2P}{\mathrm{d}x_1^2} - aP - \dfrac{\mathrm{d}\xi}{\mathrm{d}x_1} = 0 & \text{in } \Omega_R \\ \dfrac{\mathrm{d}}{\mathrm{d}x_1}\left(-\dfrac{\mathrm{d}\xi}{\mathrm{d}x_1}\right) + \dfrac{1}{\varepsilon_0}\dfrac{\mathrm{d}P}{\mathrm{d}x_1} + \dfrac{\xi}{\lambda^2} = \dfrac{q}{\varepsilon_0\beta}\left(\phi - \hat{\mu} - \alpha_{el}\dfrac{\mathrm{d}u}{\mathrm{d}x_1}\right) & \text{in } \Omega_R \end{cases} \tag{52}$$

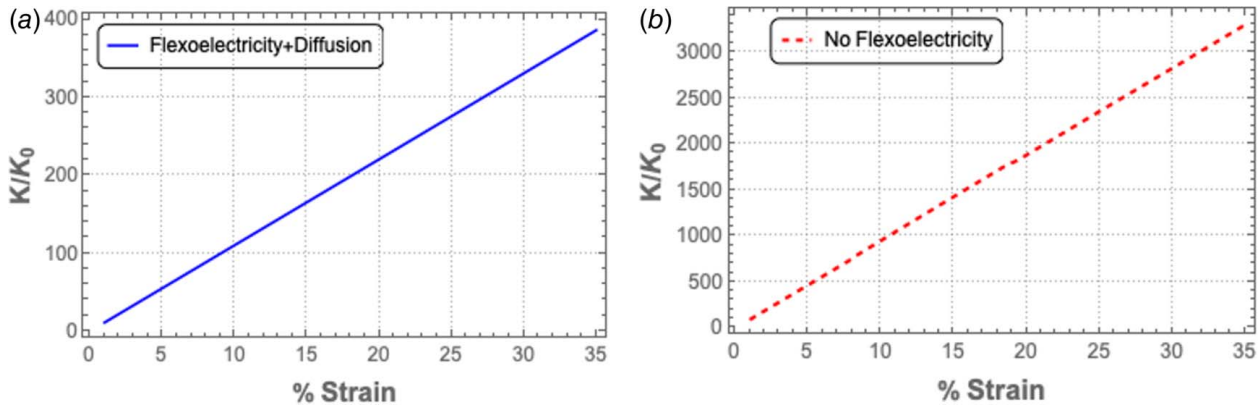

Fig. 4 Normalized ionic conductivity of a thin film of thickness 50 nm as a function of uniaxial strain for (*a*) an electro-elastic-diffusive system with flexoelectricity and (*b*) an electro-diffusive system without flexoelectricity

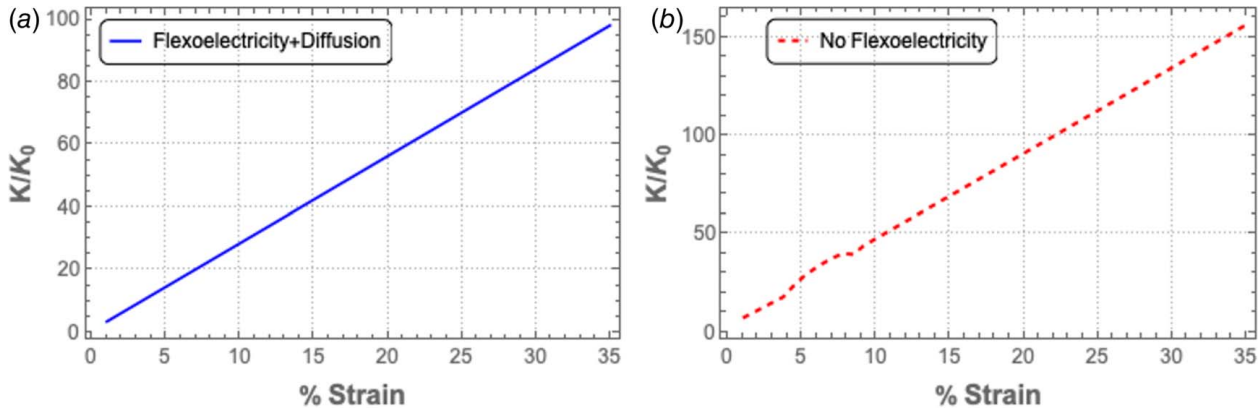

Fig. 5 Normalized ionic conductivity of a thin film of thickness 100 nm as a function of uniaxial strain for (*a*) an electro-elastic-diffusive system with flexoelectricity and (*b*) an electro-diffusive system without flexoelectricity

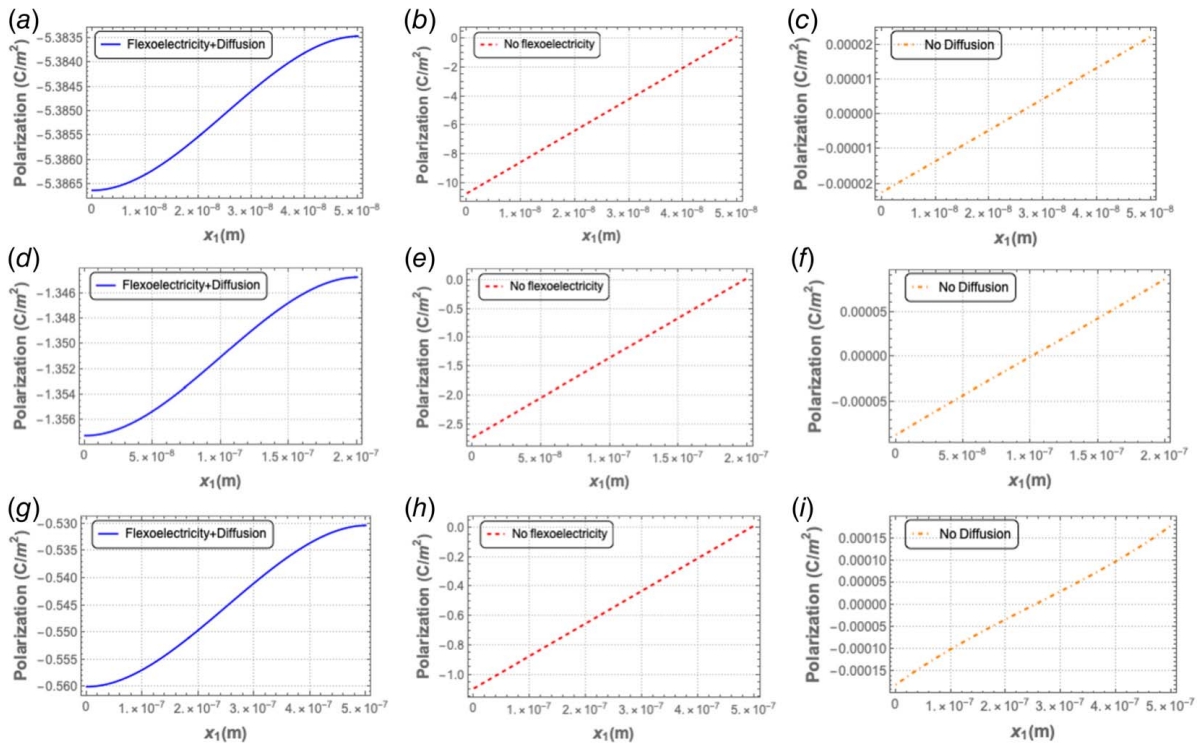

Fig. 6 Variation of polarization along the thickness direction for a thin film for three systems—electro-elastic-diffusive system with flexoelectricity (left), electro-diffusive system without flexoelectricity (center), and electromechanical system with flexoelectricity without diffusion (right). Plots (*a*), (*b*), and (*c*) show polarization for a 50 nm thin sheet. Likewise, plots (*d*), (*e*), and (*f*) show polarization for a 200 nm thin sheet, while plots (*g*), (*h*), and (*i*) show polarization for a 500 nm thin sheet.

Here, $h = e - f$. Finally, assuming open circuit conditions, i.e., $\phi = 0$, the governing equations take the form

$$\begin{cases} \dot{c} = 0, \quad J = -c\gamma\nabla\phi & \text{in} \quad \Omega_R \\ \left(\mathbb{C} - \dfrac{\alpha_{el}^2}{\beta}\right)\dfrac{\mathrm{d}^2u}{\mathrm{d}x_1^2} + h\dfrac{\mathrm{d}^2P}{\mathrm{d}x_1^2} + \dfrac{\alpha_{el}}{\beta}\dfrac{\mathrm{d}\mu}{\mathrm{d}x_1} = 0 & \text{in} \quad \Omega_R \\ h\dfrac{\mathrm{d}^2u}{\mathrm{d}x_1^2} + b\dfrac{\mathrm{d}^2P}{\mathrm{d}x_1^2} - aP + \dfrac{1}{q}\dfrac{\mathrm{d}\mu}{\mathrm{d}x_1} = 0 & \text{in} \quad \Omega_R \\ \dfrac{\mathrm{d}^2\mu}{\mathrm{d}x_1^2} + \dfrac{q}{\varepsilon_0}\dfrac{\mathrm{d}P}{\mathrm{d}x_1} - \dfrac{\mu}{\lambda^2} = -\dfrac{1}{\lambda^2}\left(\hat{\mu} + \alpha_{el}\dfrac{\mathrm{d}u}{\mathrm{d}x_1}\right) & \text{in} \quad \Omega_R \end{cases} \tag{53}$$

3.2 Boundary Conditions. We apply the following boundary conditions:

(1) Assuming $\bar{\varepsilon}$ to be the average normal strain in the film, the displacements at the top and bottom of the film are given as

$$u|_{x_1=w} - u|_{x_1=0} = w\bar{\varepsilon} \tag{54}$$

(2) The electric tensor, Λ, is specified to be zero at both ends of the film. The electric tensor, conjugate to the polarization gradient, is defined as

$$\Lambda = \frac{\mathrm{d}\Psi}{\mathrm{d}\Pi} = e\frac{\mathrm{d}u}{\mathrm{d}x_1} + b\frac{\mathrm{d}P}{\mathrm{d}x_1} \tag{55}$$

Hence, the boundary conditions are given by

$$e\frac{\mathrm{d}u}{\mathrm{d}x_1}\bigg|_{x_1=w} + b\frac{\mathrm{d}P}{\mathrm{d}x_1}\bigg|_{x_1=w} = 0 \tag{56}$$

$$e\frac{\mathrm{d}u}{\mathrm{d}x_1}\bigg|_{x_1=0} + b\frac{\mathrm{d}P}{\mathrm{d}x_1}\bigg|_{x_1=0} = 0 \tag{57}$$

(3) The chemical potential μ and its derivative μ' are prescribed on the boundaries as follows:

$$\mu|_{x_1=0} = \mu_0 \tag{58}$$

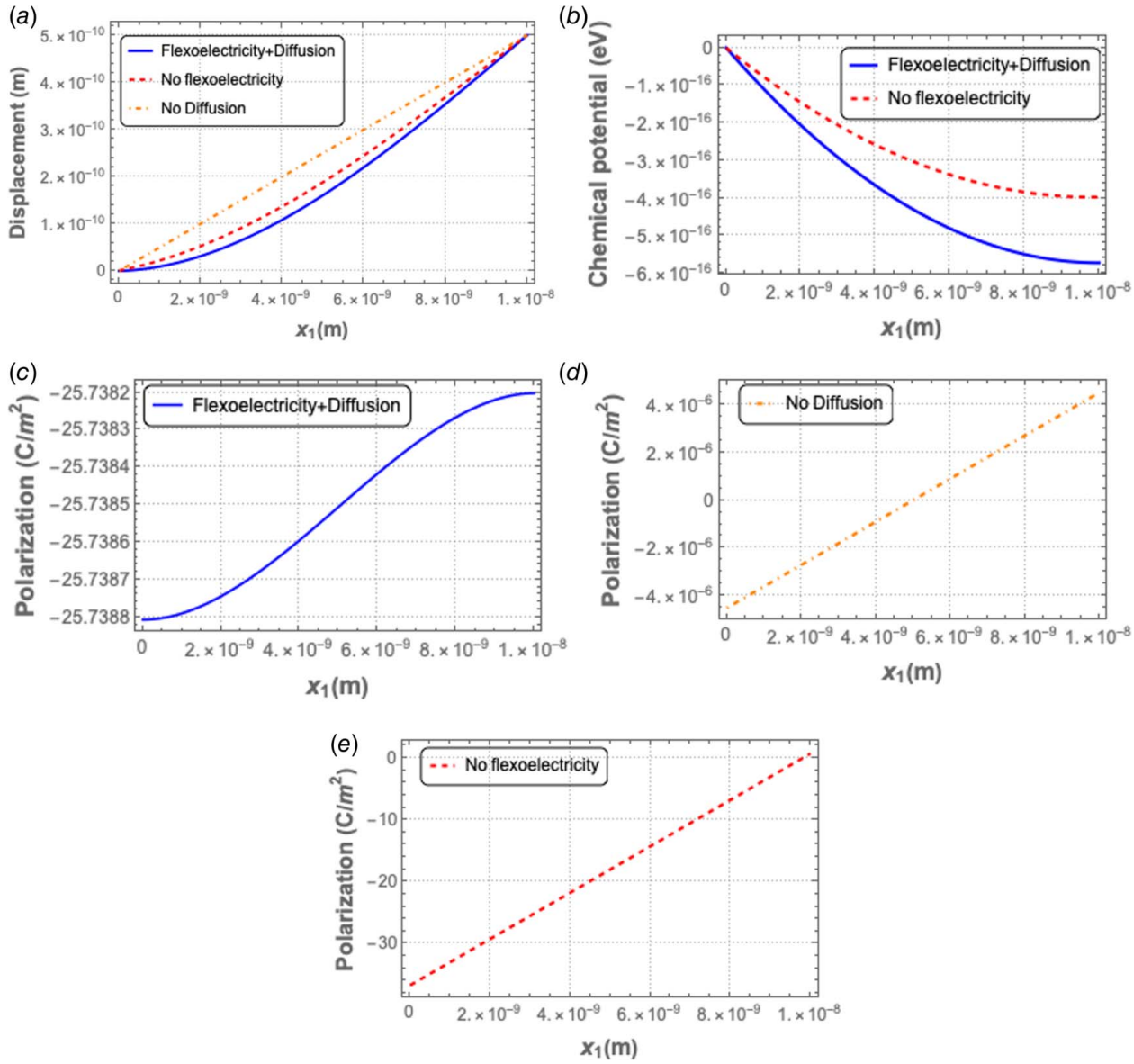

Fig. 7 Displacement, polarization, and chemical potential plotted along the thickness direction for a 10 nm thin film for three cases—electro-elastic-diffusive system with flexoelectricity, electro-diffusive system without flexoelectricity, and flexoelectric system without diffusion. (*a*) Compares the displacements for the three systems. (*b*) Compares the chemical potential between the electro-elastic-diffusive system with flexoelectricity and without. (*c*), (*e*), and (*d*) The polarization along the thickness direction for the three systems, respectively.

$$\mu'|_{x_1=w} - \mu'|_{x_1=0} = qE \tag{59}$$

where E is the applied electric field.

4 Results and Discussion

In this section, we present our results for the electro-chemo-mechanical behavior of a polymer thin film by solving the boundary value problem derived in the previous section. We chose PVDF as the material for the thin film. The material properties for PVDF are mentioned in Appendix B. The governing equations in Eq. (53) are solved for the boundary conditions in Eqs. (54)–(59) using the NDSolve package in Mathematica [44] for a fully coupled electromechanical diffusive system. We also solve the boundary value problem for two more cases to facilitate a comparative study of the different effects—electromechanical coupling with diffusion but without flexoelectricity (this reduces to the model proposed by Mozaffari et al. [38]) and electromechanical coupling with flexoelectricity but without diffusion (this reduces to a one-dimensional system based on the theory presented by Deng et al. [39]).

Figure 3 shows the variation of the normalized ionic conductivity with the film thickness under the effect of flexoelectricity and diffusion at 5% uniaxial strain. The ionic conductivity is calculated based on the solution for concentration $c(x_1)$ using the expression derived by Mozaffari et al. [38]. For convenience, we have summarized the derivation in Appendix A. We observe that the ionic conductivity increases exponentially as the film thickness approaches the Debye length for PVDF which is about 4 nm. The ionic conductivity rapidly approaches the bulk value when the film thickness is greater than 200 nm. We note that the lengthscale introduced by flexoelectricity is on the same order as the radius of gyration which is about 280 nm for PVDF.

To isolate the effect of flexoelectricity on the ionic conductivity, we plot the normalized ionic conductivity as a function of strain for a 50 nm and a 100 nm thin film as shown in Figs. 4 and 5, respectively. We make two observations here. For a 50 nm thin film, the ionic conductivity in the absence of flexoelectricity is almost tenfold higher than in the case with flexoelectricity (Figs. 4(*a*) and 4(*b*)). This indicates that for the particular boundary value problem studied here, flexoelectricity appears to reduce the ionic conductivity dramatically. However, for a 100 nm thin film, the ionic conductivity in the absence of flexoelectricity is only slightly greater than in the case with flexoelectricity (Figs. 5(*a*) and 5(*b*)). Taken together, Figs. 4 and 5 reveal that flexoelectricity has a much greater impact on ionic conductivity at small film thickness and has no effect when the film thickness is on the order of the flexoelectricity lengthscale and larger.

The reason for this rather unexpected effect of flexoelectricity on ionic conductivity can be illustrated using Fig. 6. It shows the polarization for a 50 nm PVDF thin film for the three different cases, namely, electro-elastic-diffusive system with flexoelectricity, electro-diffusive system without flexoelectricity, and flexoelectric system without diffusion. Since our boundary conditions dictate that the chemical potential at $x_1 = 0$ is higher than that at $x_1 = w$, ions flow from the bottom to the top of the film. Hence, as shown in Fig. 6(*b*), the polarization due to the diffusion of ions is negative, that is, acting in the downward direction, opposite to the flow of ions. Moreover, it increases in magnitude from the top surface to the bottom surface. In contrast, Fig. 6(*c*) shows that the net polarization due to flexoelectricity in the absence of diffusion of ions is zero. Nevertheless, Fig. 6(*a*) reveals that under the combined effect of flexoelectricity and diffusion, polarization is negative and almost constant through the film thickness. This implies that the total polarization induced by flexoelectricity and diffusion is more complex than simply adding the polarization due to the two phenomena. Moreover, the polarization induced by flexoelectricity creates a resistance to the flow of ions which in turn reduces the ionic conductivity.

Figure 7 shows the results for displacement, chemical potential, and polarization obtained for a film thickness of 10 nm at 5% strain. The plots shown in Fig. 7(*a*) for displacement and Fig. 7(*d*) for polarization due to flexoelectric effect without diffusion are consistent with the results for a thin film with flexoelectricity presented by Sharma et al. [45].

5 Conclusion

In this paper, we present a nonlinear continuum theory that integrates mechanical, electrical, and chemical coupled phenomena in flexoelectric-elastic-diffusive systems. By combining elements from existing literature on continuum mechanics of electro-elastic-diffusive systems and the theory of flexoelectricity, our study bridges the gap between these theories to present a nonlinear electro-chemo-mechanical theory incorporating flexoelectricity for soft materials. By applying this theoretical framework to a specific boundary problem of a thin film, we gain insights into the effect of the coupling of flexoelectricity and diffusion on the ionic conductivity of thin films made of soft materials. The thin film example reveals that flexoelectricity can have a dramatic impact on ionic conductivity due to the interplay between the polarization induced by the flexoelectric effect and the flow of ions. Although our theoretical formulation is general, we chose a simple one-dimensional boundary value problem to demonstrate its application to soft solid electrolytes. The proposed theory can open avenues for further investigations into complex systems which would have real-world applications specifically in the field of energy harvesting or electromechanical phenomena in biological systems where flexoelectricity plays a vital role.

Acknowledgment

The authors thank Professor Pradeep Sharma and Dr. Kosar Mozaffari for insightful discussions. The authors also gratefully acknowledge the support of NSF under grant DMR-2210155 and the Bill D. Cook Professorship.

Conflict of Interest

There are no conflicts of interest.

Data Availability Statement

The authors attest that all data for this study are included in the paper.

Appendix A. Derivation of Ionic Conductivity

Here, we summarize the approximate expression for ionic conductivity derived in Ref. [38]. As shown in Fig. 8, let the single layer be subjected to the electrochemical potential, chemical potential, and electric potential denoted by $\nabla\phi$, $\nabla\mu$, and $\nabla\xi$ at the ends of

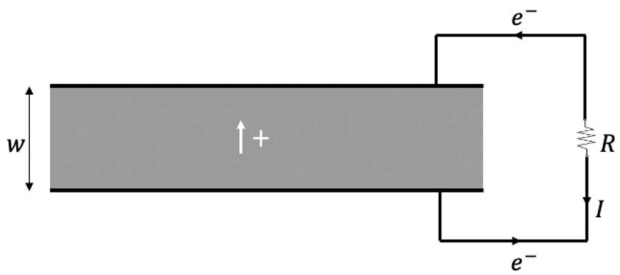

Fig. 8 Schematic of a single layer of electrolyte of width *w*. The direction of the flow of positive ions is shown by the white arrow.

the electrolyte, respectively. Let the resistance in the external circuit be R. The total current in the external circuit is given by $I = \Delta\xi/R$. J is the ionic flux which is given by the expression $J = I/qA$. Here, A is the normal surface area of the contact electrode with the electrolyte. Ionic conductivity K satisfies the equation

$$J = -K\frac{\nabla\phi}{w} \tag{A1}$$

From Eq. $(53)_1$, we get the following equation which gives a representation of K in terms of ionic concentration:

$$\nabla\phi = -\frac{Jw}{K} = -\int_0^w \frac{J}{\gamma c(x)} \tag{A2}$$

Substituting the above equation in Eq. (A1), we get the expression for ionic conductivity

$$K = \left[\frac{1}{w}\int_0^w \frac{J}{\gamma c(x)}\,\mathrm{d}x\right]^{-1} \tag{A3}$$

Appendix B. Material Properties for PVDF

The values are summarized in Table 1. The expression $\left(b\mathbb{C} - h^2\right)\varepsilon_0/\mathbb{C}(1 + a\varepsilon_0)$ has the same order as the radius of gyration (2.8×10^{-7} m). The value of the parameter b thus is estimated using this relation as 9.927×10^{-3} N m^4/C^2. The order of e and f are the same as they occur only simultaneously in the governing equations. The initial concentration is taken as 50 mol and the chemical potential of pure ion is taken as 0.5 eV [38]. The flexoelectric coefficients and Young's modulus are taken from Refs. [28,46], respectively. Refer to Refs. [38,47] for the numerical values for diffusion-related material constants.

Table 1 Material properties of PVDF used in this example

Serial No.	Parameter	Value and units
1	b	9.927×10^{-3} N m^4/C^2
2	c	3.7 GPa
3	f	−179 N m/C
4	a	1.38×10^{10} N m^2/C^2
5	ε_r	10
6	ε_0	8.854×10^{-12} C^2/N m^2
7	μ_0	0 eV
8	$\hat{\mu}$	0.5 eV
9	λ_r	4×10^{-9} m
10	α_{el}	4×10^{-9} J
11	β	$\sqrt{q^2\lambda^2/\varepsilon_r\varepsilon_0} = 4.62 \times 10^{-46}$ N$^{1/2}$ m^2
12	q	1.6×10^{-19} C
13	c_0	50 mol
14	γ	1000 m^2/V s

Note: Here, $\lambda_r\left(=\lambda\sqrt{\varepsilon_r}\right)$ is the Debye length for PVDF, γ is the mobility, and c_0 is the initial concentration.

References

[1] Zito, R., and Ardebili, H., 2019, *Energy Storage: A New Approach*, Wiley-Scrivener, Beverly, CA.

[2] Lukatskaya, M. R., Dunn, B., and Gogotsi, Y., 2016, "Multidimensional Materials and Device Architectures for Future Hybrid Energy Storage," Nat. Commun., **7**(1), p. 12647.

[3] Park, S., Heo, S. W., Lee, W., Inoue, D., Jiang, Z., Yu, K., Jinno, H., et al., 2018, "Self-Powered Ultra-Flexible Electronics Via Nano-Grating-Patterned Organic Photovoltaics," Nature, **561**(7724), pp. 516–521.

[4] Yang, Y., 2020, "A Mini-review: Emerging All-Solid-State Energy Storage Electrode Materials for Flexible Devices," Nanoscale, **12**(6), pp. 3560–3573.

[5] Di Leo, C. V., Rejovitzky, E., and Anand, L., 2014, "A Cahn-Hilliard-Type Phase-Field Theory for Species Diffusion Coupled With Large Elastic Deformations: Application to Phase-Separating Li-Ion Electrode Materials," J. Mech. Phys. Solids, **70**(Oct.), pp. 1–29.

[6] Sethuraman, V. A., Chon, M. J., Shimshak, M., Srinivasan, V., and Guduru, P. R., 2010, "In Situ Measurements of Stress Evolution in Silicon Thin Films During Electrochemical Lithiation and Delithiation," J. Power Sources, **195**, pp. 5062–5066.

[7] Bower, A., Guduru, P., and Sethuraman, V., 2011, "A Finite Strain Model of Stress, Diffusion, Plastic Flow, and Electrochemical Reactions in a Lithium-Ion Half-Cell," J. Mech. Phys. Solids, **59**(4), pp. 804–828.

[8] Gao, F., and Hong, W., 2016, "Phase-Field Model for the Two-Phase Lithiation of Silicon," J. Mech. Phys. Solids, **94**, pp. 18–32.

[9] Pharr, M., Suo, Z., and Vlassak, J. J., 2013, "Measurements of the Fracture Energy of Lithiated Silicon Electrodes of Li-Ion Batteries," Nano Lett., **13**(11), pp. 5570–5577.

[10] Mendez, J., Ponga, M., and Ortiz, M., 2018, "Diffusive Molecular Dynamics Simulations of Lithiation of Silicon Nanopillars," J. Mech. Phys. Solids, **115**, pp. 123–141.

[11] Xu, S., Zhang, Y., Cho, J., Lee, J., Huang, X., Jia, L., Fan, J. A., et al., 2013, "Stretchable Batteries With Self-similar Serpentine Interconnects and Integrated Wireless Recharging Systems," Nat. Commun., **4**(1), p. 1543.

[12] Kammoun, M., Berg, S., and Ardebili, H., 2015, "Flexible Thin-Film Battery Based on Graphene-Oxide Embedded in Solid Polymer Electrolyte," Nanoscale, **7**, pp. 17516–17522.

[13] Ganser, M., Hildebrand, F. E., Kamlah, M., and McMeeking, R. M., 2019, "A Finite Strain Electro-Chemo-Mechanical Theory for Ion Transport With Application to Binary Solid Electrolytes," J. Mech. Phys. Solids, **125**, pp. 681–713.

[14] Deshpande, V. S., and McMeeking, R. M., 2023, "Models for the Interplay of Mechanics, Electrochemistry, Thermodynamics, and Kinetics in Lithium-Ion Batteries," Appl. Mech. Rev., **75**(1), p. 010801.

[15] Winter, M., and Brodd, R. J., 2004, "What Are Batteries, Fuel Cells, and Supercapacitors?" Chem. Rev., **104**(10), pp. 4245–4270.

[16] Goodenough, J. B., and Park, K.-S., 2013, "The Li-Ion Rechargeable Battery: A Perspective," J. Am. Chem. Soc., **135**(4), pp. 1167–1176.

[17] Yang, H., and Wu, N., 2022, "Ionic Conductivity and Ion Transport Mechanisms of Solid-State Lithium-Ion Battery Electrolytes: A Review," Energy Sci. Eng., **10**(5), pp. 1643–1671.

[18] Manthiram, A., Yu, X., and Wang, S., 2017, "Lithium Battery Chemistries Enabled by Solid-State Electrolytes," Nat. Rev. Mater., **2**(4), pp. 1–16.

[19] Li, C., Wang, Z.-Y., He, Z.-J., Li, Y.-J., Mao, J., Dai, K.-H., Yan, C., and Zheng, J.-C., 2021, "An Advance Review of Solid-State Battery: Challenges, Progress and Prospects," Sustain. Mater. Technol., **29**, p. e00297.

[20] Koyama, Y., Chin, T. E., Rhyner, U., Holman, R. K., Hall, S. R., and Chiang, Y.-M., 2006, "Harnessing the Actuation Potential of Solid-State Intercalation Compounds," Adv. Funct. Mater., **16**(4), pp. 492–498.

[21] Liu, L., Xu, J., Wang, S., Wu, F., Li, H., and Chen, L., 2019, "Practical Evaluation of Energy Densities for Sulfide Solid-State Batteries," ETransportation, **1**, p. 100010.

[22] Rui, X., Ren, D., Liu, X., Wang, X., Wang, K., Lu, Y., Li, L., et al., 2023, "Distinct Thermal Runaway Mechanisms of Sulfide-Based All-Solid-State Batteries," Energy Environ. Sci., **16**(8), pp. 3552–3563.

[23] Kezuka, K., Hatazawa, T., and Nakajima, K., 2001, "The Status of Sony Li-Ion Polymer Battery," J. Power Sources, **97**, pp. 755–757.

[24] Yu, Z., Zhang, X., Fu, C., Wang, H., Chen, M., Yin, G., Huo, H., and Wang, J., 2021, "Dendrites in Solid-State Batteries: Ion Transport Behavior, Advanced Characterization, and Interface Regulation," Adv. Energy Mater., **11**(18), p. 2003250.

[25] Ardebili, H., 2019, "A Perspective on the Mechanics Issues in Soft Solid Electrolytes and the Development of Next-Generation Batteries," J. Appl. Mech., **87**(Nov.), p. 040801.

[26] Krichen, S., and Sharma, P., 2016, "Flexoelectricity: A Perspective on an Unusual Electromechanical Coupling," J. Appl. Mech., **83**(3), p. 030801.

[27] Deng, Q., Liu, L., and Sharma, P., 2014, "Flexoelectricity in Soft Materials and Biological Membranes," J. Mech. Phys. Solids, **62**, pp. 209–227.

[28] Chu, B., and Salem, D., 2012, "Flexoelectricity in Several Thermoplastic and Thermosetting Polymers," Appl. Phys. Lett., **101**(10), p. 103905.

[29] Grasinger, M., Mozaffari, K., and Sharma, P., 2021, "Flexoelectricity in Soft Elastomers and the Molecular Mechanisms Underpinning the Design and Emergence of Giant Flexoelectricity," Proc. Natl. Acad. Sci. USA, **118**(21), p. e2102477118.

[30] Petrov, A. G., 2002, "Flexoelectricity of Model and Living Membranes," Biochim. Biophys. Acta–Biomembr., **1561**(1), pp. 1–25.

[31] Petrov, A., 1984, "Flexoelectricity of Lyotropics and Biomembranes," Il Nuovo Cimento D, **3**, pp. 174–192.

[32] Liu, L. P., and Sharma, P., 2013, "Flexoelectricity and Thermal Fluctuations of Lipid Bilayer Membranes: Renormalization of Flexoelectric, Dielectric, and Elastic Properties," Phys. Rev. E, **87**, p. 032715.

[33] Mohammadi, P., Liu, L., and Sharma, P., 2014, "A Theory of Flexoelectric Membranes and Effective Properties of Heterogeneous Membranes," J. Appl. Mech., **81**(1), p. 011007.

[34] Torbati, M., Mozaffari, K., Liu, L., and Sharma, P., 2022, "Coupling of Mechanical Deformation and Electromagnetic Fields in Biological Cells," Rev. Mod. Phys., **94**(May), p. 025003.

[35] Mozaffari, K., Ahmadpoor, F., Deng, Q., and Sharma, P., 2023, "A Minimal Physics-Based Model for Musical Perception," Proc. Natl. Acad. Sci. USA, **120**(5), p. e2216146120.

[36] Buka, A., and Éber, N., 2013, *Flexoelectricity in Liquid Crystals: Theory, Experiments and Applications*, Imperial College Press, London.

[37] Meyer, R. B., 1969, "Piezoelectric Effects in Liquid Crystals," Phys. Rev. Lett., **22**(18), p. 918.

[38] Mozaffari, K., Liu, L., and Sharma, P., 2022, "Theory of Soft Solid Electrolytes: Overall Properties of Composite Electrolytes, Effect of Deformation and

Microstructural Design for Enhanced Ionic Conductivity," J. Mech. Phys. Solids, **158**, p. 104621.
[39] Deng, Q., Liu, L., and Sharma, P., 2017, "A Continuum Theory of Flexoelectricity," *Flexoelectricity in Solids: From Theory to Applications*, A. K. Tagantsev and P. V. Yudin, eds., World Scientific, Hackensack, NJ, pp. 111–167.
[40] Anand, L., 2012, "A Cahn–Hilliard-Type Theory for Species Diffusion Coupled With Large Elastic–Plastic Deformations," J. Mech. Phys. Solids, **60**(12), pp. 1983–2002.
[41] Darbaniyan, F., Dayal, K., Liu, L., and Sharma, P., 2019, "Designing Soft Pyroelectric and Electrocaloric Materials Using Electrets," Soft Matter, **15**(2), pp. 262–277.
[42] Mindlin, R. D., 1968, "Polarization Gradient in Elastic Dielectrics," Int. J. Solids Struct, **4**(6), pp. 637–642.
[43] Zheng, Q., and Wei, G.-W., 2011, "Poisson–Boltzmann–Nernst–Planck Model," J. Chem. Phys., **134**(19), p. 194101.
[44] W. R. Inc., 2023, "Mathematica, Version 13.3," Champaign, IL.
[45] Sharma, N., Landis, C., and Sharma, P., 2010, "Piezoelectric Thin-Film Superlattices Without Using Piezoelectric Materials," J. Appl. Phys., **108**(2), p. 024304.
[46] Guney, H. Y., 2005, "Elastic Properties and Mechanical Relaxation Behaviors of PVDF (Poly (Vinylidene Fluoride)) at Temperatures Between 20 and 100 °C and at 2 MHz Ultrasonic Frequency," J. Polym. Sci. Part B: Polym. Phys., **43**(20), pp. 2862–2873.
[47] Deng, Q., Kammoun, M., Erturk, A., and Sharma, P., 2014, "Nanoscale Flexoelectric Energy Harvesting," Int. J. Solids Struct., **51**(18), pp. 3218–3225.